Journal of Controlled Release 331 (2021) 364–375

Contents lists available at ScienceDirect

Journal of Controlled Release

journal homepage: www.elsevier.com/locate/jconrel

Zwitterionic self-assembled nanoparticles as carriers for *Plasmodium* targeting in malaria oral treatment

Arnau Biosca [a,b,c,1], Pol Cabanach [d,1], Muthanna Abdulkarim [e], Mark Gumbleton [e], Cristian Gómez-Canela [f], Miriam Ramírez [a], Inés Bouzón-Arnáiz [a,b,c], Yunuen Avalos-Padilla [a,b,c], Salvador Borros [d,**], Xavier Fernàndez-Busquets [a,b,c,*]

[a] Barcelona Institute for Global Health (ISGlobal, Hospital Clínic-Universitat de Barcelona), Rosselló 149-153, ES-08036 Barcelona, Spain
[b] Nanomalaria Group, Institute for Bioengineering of Catalonia (IBEC), The Barcelona Institute of Science and Technology, Baldiri Reixac 10-12, ES-08028 Barcelona, Spain
[c] Nanoscience and Nanotechnology Institute (IN2UB), University of Barcelona, Martí i Franquès 1, ES-08028 Barcelona, Spain
[d] Grup d'Enginyeria de Materials (GEMAT), Institut Químic de Sarrià, Universitat Ramon Llull, Via Augusta 390, 08017 Barcelona, Spain
[e] School of Pharmacy & Pharmaceutical Sciences, Cardiff University, Cardiff, UK
[f] Departament de Química Analítica, Institut Químic de Sarrià, Universitat Ramon Llull, Via Augusta 390, 08017 Barcelona, Spain

ARTICLE INFO

Keywords:
Plasmodium
Malaria
PBMA-MESBMA
Zwitterionic block copolymers
Curcumin
Drug delivery

ABSTRACT

The current decline in antimalarial drug efficacy due to the evolution of resistant *Plasmodium* strains calls for new strategies capable of improving the bioavailability of antimalarials, especially of those whose lipophilic character imparts them a low solubility in biological fluids. Here we have designed, synthesized and characterized amphiphilic zwitterionic block copolymers forming nanoparticles capable of penetrating the intestinal epithelium that can be used for oral administration. Poly(butyl methacrylate-*co*-morpholinoethyl sulfobetaine methacrylate) (PBMA-MESBMA)-based nanoparticles exhibited a specific targeting to *Plasmodium falciparum*-infected vs. parasite-free red blood cells (74.8%/0.8% respectively), which was maintained upon encapsulation of the lipophilic antimalarial drug curcumin (82.6%/0.3%). The in vitro efficacy of curcumin upon encapsulation was maintained relative to the free compound, with an IC50 around 5 μM. In vivo assays indicated a significantly increased curcumin concentration in the blood of mice one hour after being orally fed PBMA-MESBMA-curcumin in comparison to the administration of free drug (18.7 vs. 2.1 ng/ml, respectively). At longer times, however, plasma curcumin concentration equaled between free and encapsulated drug, which was reflected in similar in vivo antimalarial activities in *Plasmodium yoelii yoelii*-infected mice. Microscopic analysis in blood samples of fluorescently labeled PBMA-MESBMA revealed the presence of the polymer inside *P. yoelii yoelii*-parasitized erythrocytes one hour after oral administration to infected animals.

1. Introduction

Encapsulation of drugs in targeted nanovectors is a rapidly growing area with a clear applicability to infectious disease treatment [1], and pharmaceutical nanotechnology has been identified as a potentially essential tool in the future fight against malaria [2,3]. The complex pathophysiology of the malaria parasite, *Plasmodium* spp., and the economic landscape of the disease are elements that call for finely tuned nanotherapies but that at the same time have to be cost-efficient. In practical terms this translates into the need for (i) safe, specific, and non-expensive targeting elements of drug-loaded nanocarriers, (ii) oral administration formulations, and, whenever possible, (iii) taking advantage of drug production resources already available by using drugs presently in decline or on hold, thus applying the 3 Rs of drug development: rescue, repurpose, and reposition. Antibody-based targeting to red blood cells (RBCs) parasitized by *Plasmodium* (pRBCs) has provided good results in improving the activity of liposome-encapsulated antimalarial drugs [4–7], which culminated in a chloroquine-encapsulating

* Corresponding author at: Barcelona Institute for Global Health (ISGlobal Hospital Clínic-Universitat de Barcelona), Rosselló 149-153, ES-08036 Barcelona, Spain.
** Corresponding author.
E-mail address: xfernandez_busquets@ub.edu (X. Fernàndez-Busquets).
[1] Both authors contributed equally.

https://doi.org/10.1016/j.jconrel.2021.01.028
Received 4 August 2020; Received in revised form 13 January 2021; Accepted 19 January 2021
Available online 23 January 2021

immunoliposomal prototype that cured malaria-infected mice upon administration of drug amounts significantly lower than those of free chloroquine required for a comparable therapeutic activity. Nevertheless, the relatively expensive and lengthy antibody production protocols have so far precluded progress of this immunoliposomal model towards preclinical assays. Alternatives to antibodies as targeting elements to pRBCs have been developed in the form of natural or synthetic polymers such as heparin and related glycosaminoglycans [8–10] or polyamidoamines [11,12], although their in vivo use is being hampered by either significant anticoagulant activity or a not sufficiently specific targeting, respectively. On the other hand, current efforts to formulate nanoparticles for oral administration of antimalarial drugs have not been fully satisfactory so far [11,13].

Over the last decade, search for antifouling and biocompatible surfaces has drawn attention among researchers in the biomedical field, since non-specific protein interactions and biofilm formation are significant problems for biosensors, medical devices and drug delivery systems [14,15]. An antifouling coating can avoid the non-specific protein adsorption of plasma proteins, the so-called protein corona, which dramatically changes the properties of nanoparticles [16,17], including a reduced targeting specificity and a fast removal from the circulation due to the stimulation of immune responses. Apart from the prevention of protein corona, antifouling nanoparticles have emerged in recent years as potential coatings for oral drug delivery systems [18]. It is thought that their properties could promote diffusion through the mucous intestinal barrier composed of negatively charged peptidoglycans with hydrophobic heads, where most drug delivery systems get entrapped [18–20]. The implementation of this technology is crucial for nanomedical applications due to the convenience and safety of oral administration in comparison to injectable drugs [21]. Different coatings with non-ionic hydrophilic materials have been broadly used in drug delivery systems to achieve biocompatible surfaces, among which poly(ethylene glycol) (PEG) stands out as the gold standard [22–24]. Since 1995, with the FDA approval of PEGylated liposomes encapsulating doxorubicin (Doxil®) as a therapy for Kaposi's sarcoma due to the increased blood circulation they provided [25], the majority of drug delivery systems brought to market make use of this polymer to enhance surface properties [23]. In 2007, Lai and coworkers discovered that PEGylated nanoparticles could diffuse through a mucous layer as they did in water [19], due to the strong hydration layer tightly coating PEGylated surfaces [26], which makes the interaction between PEG and proteins/peptidoglycans not favorable enough to displace the thermodynamically stable water layer. This suggested that PEGylation could be used to endow nanoparticles with the potential for intestinal absorption.

However, the amphiphilicity of PEG [27] induces the destabilization of liposomes and other nanoparticles due to the loss of polarity of the aqueous phase [28] and the decrease of the hydration level of hydrophilic groups [29], a drawback that, for liposomes, can be minimized by incorporating cholesterol to confer stability [30]. In addition, other major inconveniences affecting PEG efficacy are the induction by PEGylated nanoparticles of a response by the immune system of mammals [31–33] and a low cellular uptake of PEGylated nanoparticles [34]. These problems stimulated the search for new antifouling materials with properties similar to those of PEG but with better performance in biocompatibility and cell penetration. In this scenario, zwitterionic polymers arise as one of the most attractive PEG substitutes [35]. Their super-hydrophilic character (imparted by the high number of charges) [36,37] combined with a neutral net charge, endow them with better antifouling properties than PEG [38–41]. Moreover, it has been recently demonstrated that this super-hydrophilicity also imparts "stealth" behavior to zwitterionic nanoparticles when injected in the bloodstream, reducing detection by the immune system and, therefore, improving blood circulation time [42–44]. Zwitterionic polymers are also attractive candidates for the production of epithelia-penetrating nanoparticles, since they have similar surface characteristics (neutral net charge but high electronic density) as mucus-penetrating viruses [45,46]. In 2016, Shan et al. [47] discovered that poly(lactic acid) functionalized with the zwitterionic phospholipid 1,2-didodecanoyl-sn-glycero-3-phosphocholine showed excellent mucus penetrating ability and also improved 4.5-fold the cell uptake compared with PEG-poly (lactic acid).

In this article we present the design, synthesis and characterization of amphiphilic zwitterionic block copolymers in the search for intestinal epithelium-penetrating nanoparticles that could be used for oral administration of antimalarial drugs. These polymers combine the advantage of zwitterionic surfaces mentioned above with the self-assembly properties of amphiphilic polymers, with capacity to produce different nano-sized structures and, in the case of micelles, with high loading capacity of hydrophobic drugs. As a proof-of-concept drug we have chosen curcumin, whose extreme insolubility in aqueous solutions [48–50] is hampering the clinical application potential of this polyphenol with proven antimalarial activity [51–54]. Curcumin-containing nanoparticles have been tested here in in vitro *Plasmodium falciparum* cultures and in oral administration assays in mice.

2. Materials and methods

2.1. Materials

Butyl methacrylate (BMA), 1,3-propanesultone, 2-dimethyl(aminoethyl) methacrylate (DMAEMA), 2-morpholinoethyl methacrylate (MEMA), azobisisobutyronitrile (AIBN), 2-cyano-2-propyl dodecyl trithiocarbonate, ciclohexylamine and all solvents were purchased from Sigma-Aldrich (Spain). Cyanine-3-maleimide (Cy3-maleimide) was purchased from Lumiprobe GmbH (Germany). Miniextruder® and all its components were purchased from Avanti Polar Lipids, Inc. (Alabaster, IL, USA). Inhibitors of BMA and DMAEMA were removed before their use with an aluminum oxide column. Ultrapure Milli-Q® water was obtained with a Milli-Q® Integral Water Purification System for Ultrapure Water from Merck-Millipore (Spain).

2.2. Synthesis of poly(butyl methacrylate-co-sulfobetaine methacrylate) (PBMA-SBMA)

To produce the first block of $PBMA_{25}$-$SBMA_{35}$, BMA (1.0 g, 7.03 mmol) was added to the chain transfer agent (CTA) 2-cyano-2-propyl dodecyl trithiocarbonate (97.2 mg, 0.28 mmol) followed by AIBN (4.6 mg, 0.028 mmol), resulting in a molar ratio BMA:CTA:AIBN of 25:1:0.1. One ml of dioxane was further added to the reaction. Oxygen in the solution was removed by three freezing/vacuum/thawing cycles, finally introducing an argon atmosphere. The solution was stirred at 70 °C and terminated after 16 h by exposing it to the room atmosphere. The resulting PBMA was precipitated in methanol and dried over vacuum, obtaining a yellow polymer. Then, DMAEMA (397 mg, 2.52 mmol) was added to $PBMA_{25}$-CTA (394 mg, 0.10 mmol) followed by AIBN (4.9 mg, 0.03 mmol) and 1 ml of dioxane for a molar proportion DMAEMA: $PBMA_{25}$-CTA:AIBN of 35:1:0.3. Oxygen was removed by three freezing/vacuum/thawing cycles and after 16 h an argon atmosphere was applied. The solution was stirred at 70 °C and terminated by exposing it to the room atmosphere. The resulting $PBMA_{25}$-$DMAEMA_{35}$ was precipitated in hexane and dried over vacuum, obtaining a pale yellow polymer. In the case of $PBMA_{12}$-$DMAEMA_{18}$, the precipitation was done with methanol/H_2O 80:20. For the sulfobetainization, $PBMA_{25}$-$DMAEMA_{35}$ (292 mg, 0.032 mmol) was dissolved in 5 ml of tetrahydrofuran (THF), and 1,3-propanesultone (264 mg, 1.95 mmol) was added. The reaction was stirred for 16 h at room temperature to obtain a gel. The product was washed with cold THF and dried over vacuum to obtain PBMA-SBMA as a powder.

2.3. Synthesis of poly(butyl methacrylate-co-morpholinoethyl sulfobetaine methacrylate) (PBMA-MESBMA)

The same synthesis as that used in PBMA-DMAEMA was performed to produce PBMA-MEMA. Sulfobetainization was performed using a 2:1 ratio of propanesultone/MEMA in THF for 7 days in reflux and was washed with cold THF to obtain PBMA-MESBMA, whose aspect depended on the length of the blocks.

2.4. Synthesis of $PBMA_{25}$-$SBMA_{35}$-Cy3 and $PBMA_{25}$-$MESBMA_{35}$-Cy3

Cy3-maleimide (1.13 mg) was dissolved in 1 ml of THF and added to a solution of 13.2 mg of $PBMA_{25}$-$DMAEMA_{35}$ dissolved in 1 ml of THF in a sealed vial. The resulting solution was degassed with a N_2 stream. Cyclohexylamine (8.5 μl) was then added to the vial. The reaction was stirred in the dark for 16 h under N_2 atmosphere. Then, THF was evaporated with a N_2 flow and, to remove cyclohexylamine, the product was washed twice with cold hexane to obtain a red precipitate, which was dissolved with 200 μl of THF before adding a solution of 12 mg of 1,3-propanesultone in 200 μl of THF. The reaction was stirred for 16 h at room temperature. The reaction turned into a red gel that was washed 3 times with cold THF, and the product was finally dried under vacuum to obtain the final $PBMA_{25}$-$SBMA_{35}$-Cy3 with a yield of 37.5% (7.7 mg). For the synthesis of $PBMA_{25}$-$MESBMA_{35}$-Cy3, the same procedure was carried out.

2.5. Production of PBMA-SBMA and PBMA-MESBMA nanoparticles

To produce zwitterionic nanoparticles, the method having a better performance was the direct dispersion of polymer in medium followed by extrusion. Briefly, 6 mg of $PBMA_{25}$-$SBMA_{35}$ were dispersed in 10 ml of phosphate buffered saline (PBS) to a final concentration of 0.6 mg/ml and stirred for 24 h. The resulting dispersion was extruded 21 times through a filter of 200 nm using an Avanti Miniextruder®, changing the filter in every extrusion. To produce PBMA-MESBMA nanoparticles, different amounts of polymer were dispersed in ultrapure water and stirred for 24 h. Size characterization was done using a Malvern Zetasizer NanoZS instrument (Malvern Instruments, UK). When experiments required the use of nanoparticles in culture medium, the polymer was dispersed for 24 h in 1 M NaCl. Then, the dispersion was centrifuged (7400 ×*g*, 5 min) and the pellet was resuspended in Milli-Q® water and centrifuged again (7400 ×*g*, 5 min). The resulting pellet was resuspended in the corresponding medium and extruded.

2.6. Curcumin encapsulation and quantification

The encapsulation of curcumin in PBMA-SBMA nanoparticles was performed by adding different volumes of a solution of curcumin (50 mg/ml) in DMSO before the extrusion step, with an incubation time of 30 min. In the case of PBMA-MESBMA nanoparticles, the loading was performed by adding curcumin directly to the micelles and vortexing until the solution became transparent again. Finally, the samples were centrifuged (7400 ×*g*, 5 min) to remove any unloaded curcumin. Curcumin-loaded PBMA-SBMA nanoparticles were lyophilized to remove water and the lyophilized powder was dissolved with ethanol. The concentration of curcumin in the resulting samples was quantified by measuring absorbance at 420 nm.

For PBMA-MESBMA nanoparticles, non-encapsulated curcumin was quantified by centrifugation of the sample (7400 ×*g*, 10 min), resuspension of the pellet in ethanol and measurement of absorbance at 420 nm.

2.7. Cryogenic transmission electron microscopy (cryo-TEM)

The preparation of frozen samples was performed in a EM-CPC vitrification system with controlled environment (Leica Microsystems, Germany). A 4 μl sample drop was placed on a copper grid coated with a perforated polymer film. The sample excess was removed by blotting with filter paper. Right after this, the grid was plunged into liquid ethane held at a temperature just above its freezing point (94 K). The vitrified sample was transferred to the microscope for analysis. The images were obtained with a JEOL JEM-2011 microscope (JEOL LTD, Tokio, Japan) operating at 120 kV. To prevent sample perturbation and the formation of crystals, the specimens were kept cool (77 K) during the transfer and the viewing procedure.

2.8. P. falciparum cultures and in vitro growth inhibition assays

P. falciparum 3D7 was grown in vitro in human RBCs of blood group type B prepared as described elsewhere [7] using previously established conditions [55]. Briefly, parasites (thawed from glycerol stocks) were cultured at 37 °C in T25 flasks (SPL Life Sciences) in Roswell Park Memorial Institute (RPMI) complete medium (containing 5 g/l Albumax II and supplemented with 2 mM glutamine) under a gas mixture of 92% N_2, 5% CO_2, and 3% O_2. Synchronized ring stage cultures were obtained by 5% sorbitol lysis [56], and the medium was changed every 2 days maintaining 3% hematocrit. For culture maintenance, parasitemia was kept below 5% late forms by dilution with RBCs. These *Plasmodium* cultures (200 μl) were plated in 96-well plates and incubated for 48 h at 37 °C in the presence of free curcumin and polymer-curcumin conjugates dissolved in RPMI. Parasitemia was determined by microscopic counting of blood smears or by flow cytometry as previously described [4].

2.9. Targeting analysis

Living *P. falciparum* cultures were incubated in complete RPMI at 37 °C for 90 min with gentle stirring in the presence of 0.6 mg/ml (or 0.15 mg/ml for time-lapse microscopy) of Cy3-labeled SBMA and MESBMA polymers. After 80 min, Hoechst 33342 nuclear stain was added at a final concentration of 2 μg/ml and cells were further incubated for another 10 min. For fluorescence microscopy, cells were washed twice with RPMI, diluted 20 times in RPMI to reach 0.15% hematocrit and transferred into a Lab-Tek®II chambered coverglass (Nunc, Thermo Fisher Scientific; catalog number 155409). Preparations were then analyzed by laser scanning confocal microscopy in either a Leica TCS SP5 microscope (63× immersion oil objective with 1.4 numerical aperture), or a ZEISS LSM 800 microscope (100× immersion oil objective). Hoechst 33342 and Cy3 were detected by excitation with 405 nm and 514 or 561 nm lasers, respectively. Emission was collected between 415 nm and 500 nm for Hoechst 33342, and between 580 nm and 680 nm for Cy3. Time-lapse images were taken every 8 s during 55 min. For flow cytometry, cells were either washed twice with RPMI or left without washing before being diluted with PBS to reach a final hematocrit of 0.03%. Preparations were then analyzed using a LSRFortessaTM flow cytometer instrument (BD Biosciences) set up with the 5 lasers, 20 parameters standard configuration. The single-cell population was selected on a forward-side scatter scattergram. Cy3 was excited using a yellow-green laser (561 nm), and its fluorescence collected through a 610/20–600 nm LP filter. Hoechst 33342 was excited with a UV laser (350 nm), and its fluorescence collected using a 450/50 nm filter.

2.10. In vivo antimalarial assays

To test the antimalarial activity of free and encapsulated curcumin, a 4-day blood suppressive test was performed as previously described [57]. Briefly, BALB/c mice were inoculated 2×10^7 red blood cells from *Plasmodium yoelii yoelii* 17XL-infected mice by intraperitoneal injection and the survival of mice was assayed for 16 days. In order to test the prophylactic activity of curcumin, treatment started 1 day before infection (day −1), and consisted of a dose of 100 mg/kg day^{-1} curcumin administered by oral delivery of 200 μl of a 10 mg/ml curcumin

solution (in free form or incorporated in PBMA-MESBMA nanoparticles) followed by identical dose administration for the next 3 days. The samples were prepared at appropriate concentrations in water and the control groups received PBS.

2.11. Determination of curcumin concentration in plasma after oral administration

BALB/c mice were fed by gavage with 200 μl of a 3% sucrose solution containing either 10 mg/ml curcumin encapsulated in PBMA-MESBMA nanoparticles or 10 mg/ml free curcumin. Two mice where used for each sample, and the same 3% sucrose solution without curcumin was used as negative control with one mice. After the gavage, 70 μl of peripheral tail blood were taken at 1, 6 and 24 h after gavage using heparinized tubes (Microvette™ CB 300LH). Immediately after each extraction, plasma was separated from cells by centrifugation (5 min, 2000 ×*g*) and 20 μl of each fraction were stored at −80 °C. When all extractions were performed, fractions were thawed and quickly mixed with 20 μl of 4% Triton X-100 before being stored again at −80 °C.

Curcumin concentration in plasma was measured by liquid chromatography with tandem mass spectrometry (LC-MS/MS) in a liquid chromatographer connected to a triple quadrupole detector (Xevo TQS, Acquity Waters, Mildford, USA) using negative electrospray ionization. The mobile phase consisted of binary mixtures of 0.1% formic acid in either water (A) or methanol (B). Gradient elution started with 90% A and 10% B during the first minute, increasing to 90% B in 4 min, held for 5 min and returned to initial conditions in 2 min. The flow rate was set at 300 μl min^{-1} and 10 μl of sample were injected. Flow injection analysis was performed to determine the optimum cone voltage to obtain the precursor ion for curcumin. Then, collision energy was optimized obtaining three intense fragment ions. The acquisition was performed in selected reaction monitoring mode using two transitions from the precursor ion to the product ion to identify each compound. The optimal parameters are displayed in Table 1. The system and data management were processed using MassLynx v4.1 software package.

2.12. In vivo determination of polymers in pRBCs after oral administration

A BALB/c mouse was inoculated intraperitoneally with 100 μl of a *P. yoelii yoelii* 17XL MRA-267 frozen stock, and after 4 days blood was extracted from the tail and the parasitemia was checked by Giemsa staining. The infected mouse was anesthetized and total blood was obtained with an intracardiac puncture in the presence of ca. 10% EDTA (*w/v*). Blood was washed (sterile PBS, 500 ×g, 10 min), reconstituted in PBS, and 100 μl of this reconstituted blood were used to inoculate intraperitoneally BALB/c mice with ca. 2×10^6 RBCs from the infected mouse. Five days post-infection, 200 μl of 1.5 mg/ml Cy3-PBMA-SBMA or 10 mg/ml Cy3-PBMA-MESBMA polymers (dissolved in PBS and Milli-Q® H_2O, respectively) were administered by oral gavage, and blood samples were taken from the tail 20 min and 1, 2, and 4 h post-administration. A control blood sample was also removed just before administration. Samples were preserved at 4 °C in sterile PBS containing 1% EDTA (*w/v*) until their microscopic analysis, for which they were diluted 1:40 in 1× PBS containing 2 μg/ml Hoechst 33342. Images were collected with a Leica TCS SP5 fluorescence confocal microscope (Mannheim, Germany) using a 63× oil immersion objective. Cy3 was excited with a 514 nm line of an Argon laser and Hoechst 33342 with a 405 nm line of a diode laser. To avoid crosstalk between the different fluorescence signals, a sequential scanning was performed.

2.13. Hemolysis tests

Mouse blood samples were collected from six-week old BALB/c mice in heparinized tubes (1000 U heparin/ml). The fresh blood samples were centrifuged at 867 ×*g* for 10 min at 4 °C and supernatant was discarded. The pellet was washed in PBS and centrifuged again to remove traces of plasma, and finally taken up in PBS. Cell concentration was determined with a hemocytometer to adjust RBC concentration at 8×10^9 cells/ml. Ten μl of this erythrocyte suspension were added to 100 μl of each polymer sample in PBS and incubated for 10 min at 37 °C. Samples were then centrifuged, the supernatant was collected, and its absorbance was measured at 540 nm with a Tecan Infinity M Plex microplate reader (Tecan Group Ltd., Switzerland). Milli-Q® water and PBS were used as positive and negative controls respectively.

2.14. Body weight loss analysis

Six-week old BALB/c mice were distributed in 5 groups ($n = 4$) and administered intravenously with the different nanoparticle preparations in PBS. The weight of each mouse was determined every day and the animals were observed carefully for signs of toxicity. Mice were euthanized at day 3 of the nanoparticle treatment.

2.15. Ethical issues

The human blood used in this work was from voluntary donors and commercially obtained from the *Banc de Sang i Teixits* (www.bancsang.net). Blood was not collected specifically for this research; the purchased units had been discarded for transfusion, usually because of an excess of blood relative to anticoagulant solution. Prior to their use, blood units underwent the analytical checks specified in the current legislation. Before being delivered to us, unit data were anonymized and irreversibly dissociated, and any identification tag or label had been removed in order to guarantee the non-identification of the blood donor. No blood data were or will be supplied, in accordance with the current Spanish *Ley Orgánica de Protección de Datos* and *Ley de Investigación Biomédica*. The blood samples will not be used for studies other than those made explicit in this research.

Mice (18–20 g) were maintained under standard environmental conditions: 20–24 °C and 12/12 h light/dark cycle, with ad libitum access to a semi-solid diet and water during the duration of the experiments. In the presence of toxic effects including, among others, >20% reduction in animal weight, aggressive and unexpected animal behavior or the presence of blood in faeces, animals were immediately anesthetized using a 100 mg/kg Ketolar plus 5 mg/kg Midazolan mixture and sacrificed by cervical dislocation. The animal care and use protocols followed adhered to the specific national and international guidelines specified in the Spanish Royal Decree 53/2013, which is based on the European regulation 2010/63/UE. The studies reported here were performed under protocols reviewed and approved by the Ethical Committee on Clinical Research from the *Hospital Clínic de Barcelona* (Reg. HCB/2018/1223, January 23, 2019).

Table 1
LC-MS/MS optimized parameters for curcumin.

Molecular formula	Mw (Da)	Precursor ion Mw (Da)	C.V. (V)	Fragment ion 1	C.E. 1 (eV)	Fragment ion 2	C.E. 2 (eV)	Fragment ion 3	C.E. 3 (eV)
$C_{21}H_{20}O_6$	363.38	367.00	21	217	9	149	18	134	31

Mw: molecular weight; C.V.: cone voltage (V); C.E.: collision energy (eV).

3. Results and discussion

3.1. Production of PBMA-SBMA nanoparticles

PBMA-SBMA was the first polymer used to form nanoparticles due to its biodegradability and ease of synthesis. Butyl methacrylate is a well characterized monomer used broadly in drug delivery systems, while sulfobetaine methacrylate is the most used sulfobetaine monomer. Sulfobetaine was the group chosen to act as zwitterionic because it maintains its zwitterionic behavior in a broad pH range (in contrast to carboxybetaine and phosphocholine) and because its synthesis is easy and scalable. To synthesize this polymer, different RAFT polymerizations were performed; this type of polymerization allows the synthesis of block copolymers with a controlled length of each block, a critical parameter for nanoparticle structure. BMA was used as monomer for the first block and DMAEMA was used as monomer for the second block. Finally, the polymer was treated with 2-propanesultone to sulfobetainize the tertiary ammonium of DMAEMA and produce the final PBMA-SBMA (Fig. 1A).

The anti-polyelectrolyte effect, a unique behavior presented by some zwitterionic polymers when dispersed in water [41,58–60], can produce in absence of counter-ions the collapse of the structure when the charges of the polymeric chains tend to compensate each other [61]. In the case of the block copolymers presented in this article, the collapse of the zwitterionic block would produce the loss of the polymer's amphiphilic behavior and, in consequence, of its capability to produce nanoparticles. This effect was confirmed for PBMA-SBMA polymers, which did not form nanoparticles when dispersed in pure water. To avoid the anti-polyelectrolyte effect, ionic salts were added to the solvent. By doing this, ions displace the interaction between polymer charges, making the polymer chains more accessible to be solvated and recovering their hydrophilicity. This effect resulted in the dispersion of the polymer in the aqueous medium. Once dispersed, an extrusion process was used to produce the nanoparticles and control their size.

The formation of nanoparticles using the method commented above confirmed the relation between the presence of ions in the solution and the hydrophilicity of the zwitterionic block.

PBMA-SBMA nanoparticles showed good stability over time (>200 h), but they collapsed upon salt removal by dialysis, which limited some characterization techniques such as zeta-potential measurements. This led to explore the development of a new type of polymers.

3.2. Production of PBMA-MESBMA nanoparticles

For the development of a type of polymers without the ion-dependence that showed PBMA-SBMA, information reported in the work of Hildebrand et al. [60] was used; namely, that the solubility of zwitterionic polymers in pure water was affected by the pendant groups of the amine due to their importance in the ionic interactions between polymer charges. It was hypothesized that, if placing on the amine a pendant group that prevented intra-chain and inter-chain interactions, the amphiphilic character of the molecule would be maintained even in the absence of counterions. For this reason, it was decided to use a zwitterionic monomer with a voluminous group in the amine. This group would, by steric impedance, prevent the interaction between the amine and the large sulfonic group that produces the collapse of the block (Fig. 1C).

MEMA was the monomer chosen to achieve the properties commented above, whereby a copolymer consisting of PBMA and PMEMA blocks was synthetized, followed by the sulfobetainization of the

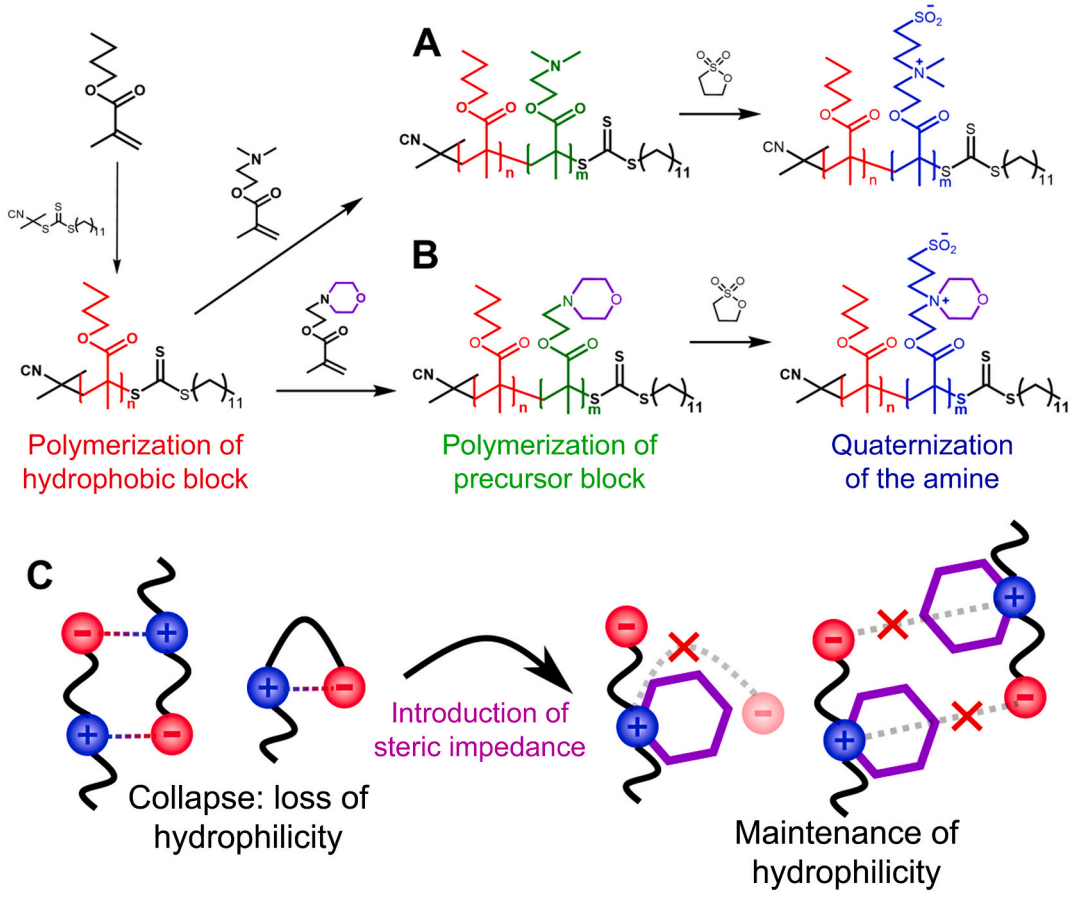

Fig. 1. Synthesis routes used to produce (A) PBMA-SBMA and (B) PBMA-MESBMA. (C) Effect of the morpholino ring in the upper critical solution temperature collapse of sulfobetaine moiety.

PMEMA block to obtain the final PBMA-MESBMA copolymer. MEMA was selected for various reasons: first, its tertiary ammonium (that will become a quaternary ammonium when sulfobetainized) is part of a ring, which will improve its steric impedance, due to its rigid structure; secondly, the ring attached to the nitrogen contains also an oxygen atom, whose presence confers hydrophilicity to the molecule. This is important because the monomer forms part of the zwitterionic block, and a hydrophobic pendant group could compromise the self-assembly of polymer molecules. Finally, MEMA is commercially available, which makes the process more cost-efficient and scalable. The synthesis of the polymer was performed as for PBMA-SBMA, with the use of MEMA as a sulfobetaine precursor instead of DMAEMA (Fig. 1B).

Once the second type of polymers were synthesized, they were used to produce nanoparticles; it was observed that when dispersed in water, the polymer did not only avoid the collapse of the hydrophilic part but also formed nanoparticles by self-assembly without the need of extrusion process. Without the ion dependency due to the addition of a voluminous group in the quaternary amine, the zwitterionic block remains hydrophilic, which allows the formation of nanoparticles in water or any other aqueous media.

Both nanoparticles produced were characterized in order to have more knowledge of the relation between the structure of the polymer and the nanoparticle morphology.

3.3. Influence of the zwitterionic group on nanoparticle structure

To determine the differences between nanoparticles formed from both polymer types, nanoparticles formed by polymers with equal block length but with different zwitterionic blocks ($PBMA_{25}$-$SBMA_{35}$ / $PBMA_{25}$-$MESBMA_{35}$) were characterized using cryo-TEM (Fig. 2). $PBMA_{25}$-$SBMA_{35}$ nanoparticles had an average diameter of ca. 100 nm, whereas nanoparticles formed by $PBMA_{25}$-$MESBMA_{35}$ showed an average diameter of ca. 20 nm. Since both nanoparticle types are produced by polymers with equal block lengths, the different sizes are determined by peculiarities in the chemical structures of the nanoparticle building blocks, each producing a distinct self-assembly.

$PBMA_{25}$-$MESBMA_{35}$ nanoparticles were formed through the direct dispersion in water of amphiphilic polymers, which led, in agreement with their size, to the self-assembly of micellar structures. On the other hand, the size and production method of $PBMA_{25}$-$SBMA_{35}$ nanoparticles are not compatible with a micellar organization; since this polymer had to be extruded to form nanoparticles, the type of amphiphilic structure that could better explain the observed properties is the polymersome, although the formation of nanocapsules would also conform to the results obtained.

Two factors are important to explain the effect of adding a voluminous group in the quaternary amine of the zwitterionic block: (i) the solvation increase induced by the reduction of interchain/intrachain interactions leads to a decrease in the hydrophilic character of the copolymer, which could exacerbate the hydrophobic effect and favor the formation of the most simple self-assembled nanoparticle; (ii) the introduction of a voluminous group can also affect the area of the hydrophilic block, producing changes in the nanoparticle structure due to steric impedance.

With the objective of evaluating the potential of amphiphilic zwitterionic block copolymers for the delivery of pRBC-targeted antimalarial drugs, we explored the in vitro targeting of PBMA-SBMA and PBMA-MESBMA nanoparticles to pRBCs. When added to cocultures of live RBCs and pRBCs, both types of nanostructures exhibited, according to flow cytometry analysis, a complete lack of interaction (<0.8%) with non-infected erythrocytes and a significant binding to *P. falciparum*-parasitized red blood cells (Fig. 3). Non-washed samples resulted in

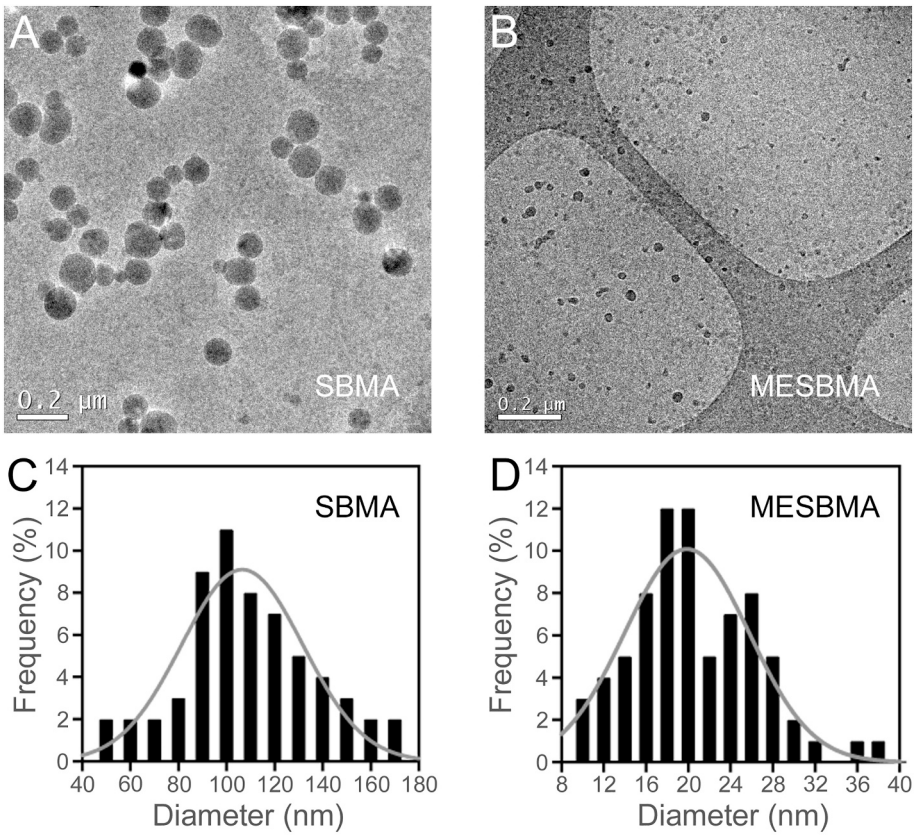

Fig. 2. Cryo-TEM images of (A) $PBMA_{25}$-$SBMA_{35}$ and (B) $PBMA_{25}$-$MESBMA_{35}$ and histograms representing nanoparticle populations of (C) $PBMA_{25}$-$SBMA_{35}$ and (D) $PBMA_{25}$-$MESBMA_{35}$; data for histograms was obtained from 10 and 6 different fields, respectively. Each bar in panels C and D represents the number of events for the corresponding bar size ±5 nm and ± 1 nm, respectively.

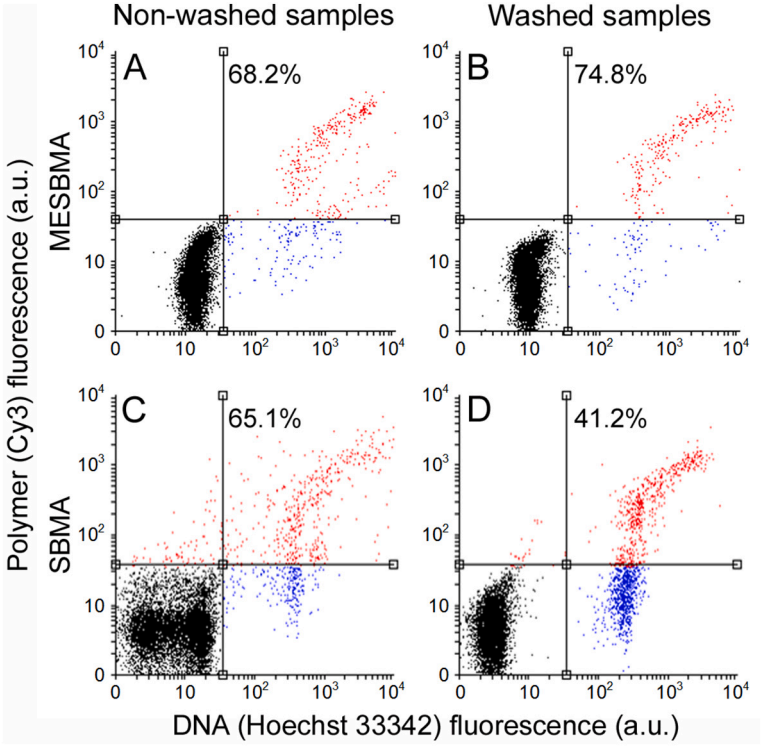

Fig. 3. Flow cytometry analysis of the interaction of Cy3-labeled PBMA-MESBMA (A,B) and PBMA-SBMA nanoparticles (C,D) with RBCs (left quadrants, no DNA content) and pRBCs (right quadrants, *Plasmodium* DNA content) in non-washed (A,C) and washed samples (B,D). Percentages indicate the fraction of polymer-bound pRBCs relative to all pRBCs. The fraction of polymer-bound RBCs relative to all RBCs was always <0.8%. a.u.: arbitrary units.

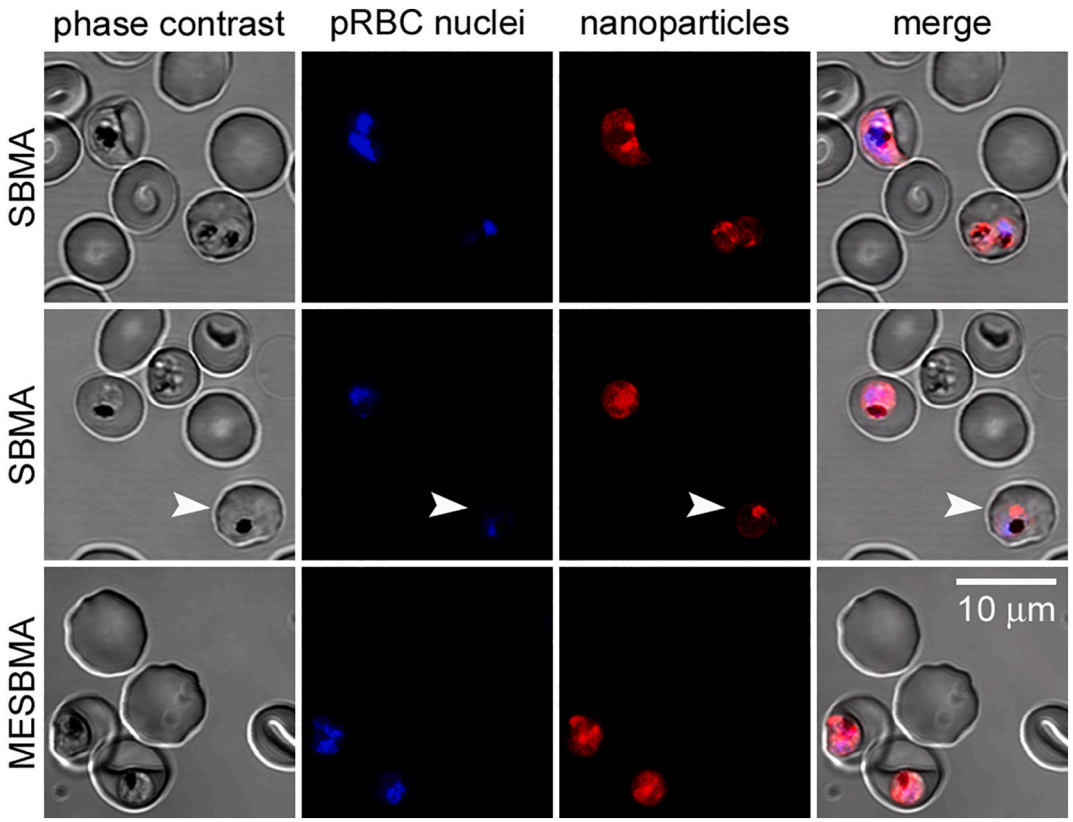

Fig. 4. Confocal fluorescence microscopy analysis of the interaction of curcumin-containing, Cy3-labeled PBMA-SBMA and PBMA-MESBMA nanoparticles with RBCs and pRBCs. The arrowhead indicates an early trophozoite-stage parasite.

>65% of pRBCs being bound to both polymers. This high fraction of targeted cells was maintained for washed PBMA-MESBMA samples, whereas for PBMA-SBMA washed samples it was reduced to ca. 40% as the washing step removed those nanoparticles that were loosely bound to the cells.

Flow cytometry results were confirmed by fluorescence confocal microscopy, where both Cy3-labeled polymers accumulated inside live intraerythrocytic parasites without detection of any significant fluorescence in the cytosol of either the host pRBC or non-parasitized erythrocytes (Fig. 4). All *P. falciparum* blood stages (rings, trophozoites and schizonts) were labeled with polymer-bound Cy3 fluorescence. Time-lapse microscopy of these living cultures (Video 1) suggested that the polymers could freely cross the plasma membranes of both pRBCs and parasites, but once inside *Plasmodium*, molecular interactions with some pathogen component(s) reduced the membrane trespassing capacity of the polymers, which remained entrapped within the parasite.

The excellent targeting specificity to pRBCs vs. RBCs of PBMA-SBMA and PBMA-MESBMA led us to explore the capacity of the polymers for the encapsulation of antimalarial drugs. Curcumin was chosen as a proof-of-concept drug due to its extremely low solubility in aqueous solvents that limits its potential as antimalarial. Curcumin encapsulation was successful in both polymers. For each mg/ml of polymer, the maximum concentration obtained of encapsulated curcumin was 40 μg/ml and 300 μg/ml for PBMA-SBMA and PBMA-MESBMA, respectively. The differences in encapsulation indicate how the self-assembly of both systems plays an important role in the capacity of nanoparticles to entrap lipophilic drugs in their hydrophobic regions, being PBMA-MESBMA the formulation with a higher curcumin solubilization capacity. The presence of encapsulated curcumin not only did not affect the pRBC binding capacity of drug-free polymers, but it actually increased to >90% of all pRBCs targeted by both structures in non-washed samples (Fig. 5). Again, washing affected significantly more the interaction with pRBCs of PBMA-SBMA/curcumin than that of PBMA-MESBMA/curcumin nanoparticles (66.1% vs. 82.6% respectively).

The good encapsulation efficiency of curcumin in nanocarriers targeted to pRBCs (vs. non-infected erythrocytes) led us to explore the antimalarial activity of encapsulated vs. free drug. The results obtained (Fig. 6) did not reveal any improvement in in vitro antimalarial drug activity imparted by its encapsulation in either nanoparticle. This result likely indicates that the amelioration conferred by an efficient targeting is masked by a slow release of curcumin from the nanoparticles.

The in vitro data were confirmed in in vivo assays where curcumin was administered to *P. yoelii yoelii*-infected mice either free or encapsulated in PBMA-MESBMA nanoparticles (Fig. 7), where no improvement in animal viability resulted from drug encapsulation relative to free curcumin. No significant hemolysis was observed for PBMA-MESBMA and PBMA-SBMA up to concentrations close to their aqueous solubility limits (10 mg/ml and 1 mg/ml respectively; Supplementary Fig. 1), whereas neither polymer induced weight loss in mice up to three days post-administration (Supplementary Fig. 2). Sulfobetainized n-butyl methacrylate-2-(dimethylamino)ethyl methacrylate copolymers have been proposed as bioinert coatings for medical devices [62], which supports the safety of this type of chemical structures for in vivo use.

Intestinal absorption following oral administration was studied for curcumin as free drug and encapsulated in PBMA-MESBMA, the polymer that was capable of encapsulating a larger amount of curcumin and which offered a better targeting to pRBCs than PBMA-SBMA. Mice were fed 200 μl of a 10 mg/ml curcumin solution either free or encapsulated, and blood samples were taken at different times for plasma curcumin determination by LC-MS/MS. At 1 h post-feeding, PBMA-MESBMA-encapsulated curcumin reached the circulation in a significantly larger concentration than the free drug (18.7 vs. 2.1 ng/ml plasma, respectively; Table 2). At longer times post-feeding the amount of curcumin in plasma increased for both formulations without remarkable quantitative differences between them.

To investigate if plasma curcumin was the result of its entry in the

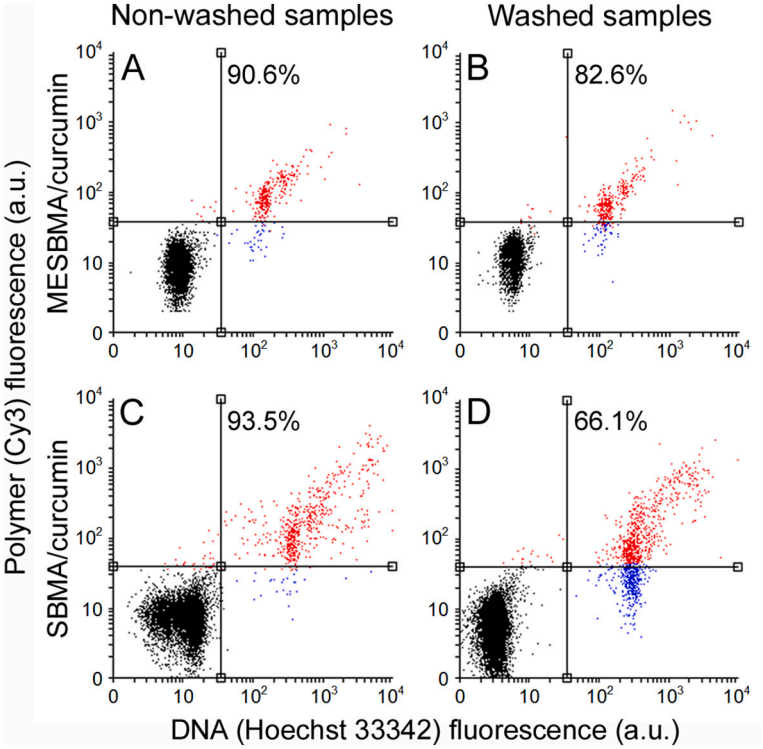

Fig. 5. Flow cytometry analysis of the interaction of Cy3-labeled, curcumin-containing, PBMA-MESBMA (A,B) and PBMA-SBMA nanoparticles (C,D) with RBCs (left quadrants, no DNA content) and pRBCs (right quadrants, *Plasmodium* DNA content) in non-washed (A,C) and washed samples (B,D). Percentages indicate the fraction of polymer-bound pRBCs relative to all pRBCs. The fraction of polymer-bound RBCs relative to all RBCs was always <0.3%. a.u.: arbitrary units.

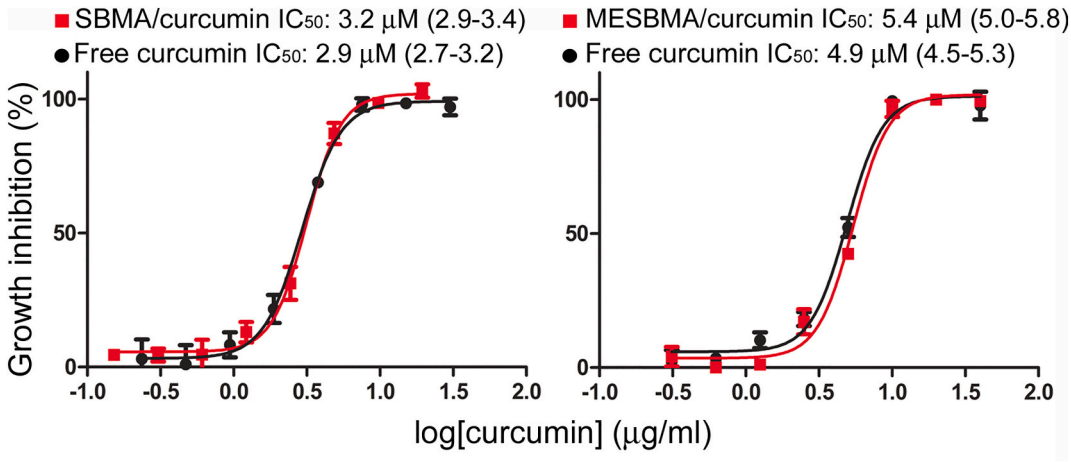

Fig. 6. Growth inhibition assays in *P. falciparum* in vitro cultures of the effect of curcumin either as free drug or encapsulated in PBMA-SBMA and PBMA-MESBMA nanoparticles.

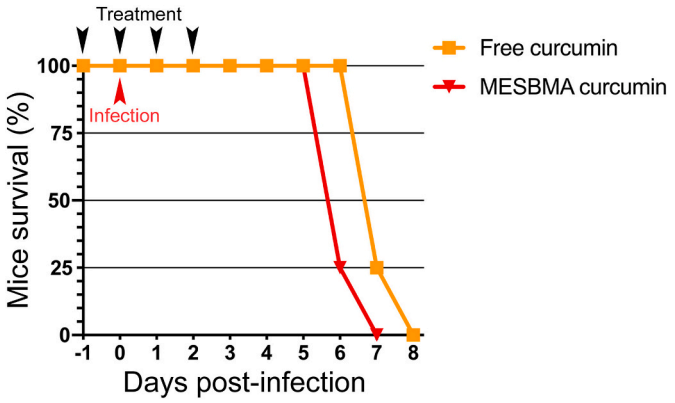

Fig. 7. Kaplan-Meier plot for the in vivo assay of the effect on *P. yoelii yoelii*-infected mice ($n = 4$ animals/sample) of free or PBMA-MESBMA-encapsulated curcumin administered orally at 100 mg/kg day^{-1}.

Table 2
LC-MS/MS determination of curcumin concentrations present at different times post-feeding in the plasma of mice orally administered with the drug either free or encapsulated in PBMA-MESBMA-based nanoparticles.

	Free curcumin		PBMA-MESBMA/curcumin	
Time (h)	Mean (ng/ml)	SD	Mean (ng/ml)	SD
1	2.1	0.9	18.7	6.2
6	21.7	2.3	17.0	0.4
24	632.4	373.9	979.6	218.6

blood circulation together with the nanoparticles or of curcumin crossing the intestinal epithelium following its dissociation from the nanocarriers in the intestinal lumen, *P. yoelii*-infected mice were fed the Cy3-labeled polymers and at different times post-administration blood samples were removed and analyzed by confocal fluorescence microscopy. The results for Cy3-PBMA-MESBMA indicated its presence inside pRBCs one hour post-administration (Fig. 8), in good correlation with the curcumin data from Table 2. On the other hand, Cy3-PBMA-SBMA could not be detected in pRBCs up to 4 h post-administration (Supplementary Fig. 3), which could be due to the significantly lower dose administered (1.5 mg/ml vs. 10 mg/ml for Cy3-PBMA-MESBMA) as a result of its poor aqueous solubility.

Curcumin has been used here as a proof-of-concept because it is inexpensive and a good model for compounds with low aqueous solubility. The majority of antimalarial drugs under development are lipophilic with poor plasma solubility and large biodistribution volumes and, consequently, with low accumulation in RBCs [4], which incurs the risk of generating resistant parasites [63–65]. As a consequence, the administration of high drug doses to the patient is required for a proper antimalarial activity, which results in an increased likelihood of causing toxic side effects. In this regard, the improved solubility of curcumin imparted by PBMA-SBMA polymers is a promising step forward towards reducing the active doses of most antimalarials.

Different types of current and future antimalarial drugs have and will likely have preferred target forms among the different *Plasmodium* blood stages [66]. Whereas many compounds are most active against late trophozoite stages, some drugs like heparin act on the invasion step that initiates the intraerythrocytic cycle [67]. Since this blood cycle is tightly synchronized in most typical malaria infections, it would be important to have access to rapid diagnostic tests offering immediate information on the most abundant stage present at a given time in a particular patient. With this personalized information available, the best stage-specific drug could be administered. However, this administration must reach the circulation as soon as possible before the stage prevalence changes. The rapid intestinal uptake provided by PBMA-MESBMA-based nanoparticles can be an important asset for future malaria therapeutic treatments using other current and future lipophilic drugs more active than curcumin.

A particularly interesting form of *Plasmodium* to be reached by drug-containing nanovectors is the ring stage corresponding to pRBCs during roughly the first half of the parasite's intraerythrocytic cycle. During this phase, the pathogen does not transform significantly the host cell membrane, which makes it difficult to distinguish parasitized from healthy erythrocytes. Indeed, mainly late-stage pRBCs are bound by drug-loaded nanocarriers decorated with a variety of targeting molecules such as antibodies [5–7], heparin [10,68], polyamidoamines [11,12], and amphiphilic dendritic derivatives [69], all of them recognizing specific membrane features of mature pRBCs. Only ligands binding receptors in all RBCs, such as antibodies against glycophorin A, are capable of also targeting ring stages [4,70]. The significant specific targeting of all pRBCs (including rings) vs. RBCs, offered especially by curcumin-loaded PBMA-MESBMA, is a relevant property of these polymers regarding their potential use in highly selective antimalarial strategies, because it will allow the delivery of drugs to the parasite early in its intraerythrocytic cycle, increasing therapeutic efficacy.

The high curcumin loading capacity of PBMA-MESBMA (0.3 mg curcumin/mg polymer) might actually lead to an underestimation of its therapeutic potential if curcumin were forming insoluble aggregated nuclei due to its high concentration inside the nanoparticles. This

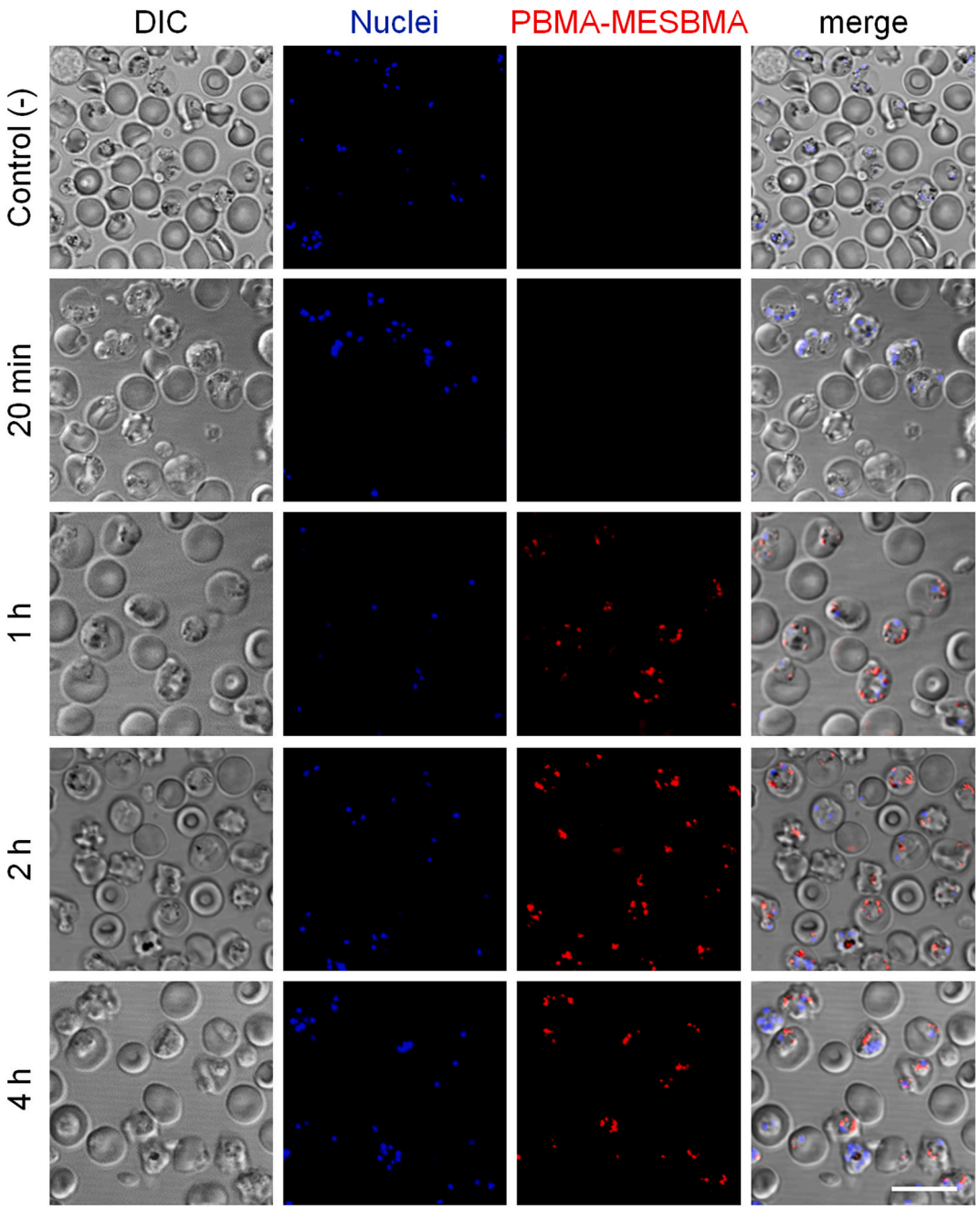

Fig. 8. Confocal fluorescence microscopy analysis of the presence of orally administered Cy3-PBMA-MESBMA in pRBCs of a *P. yoelii*-infected mouse. After blood removal at the indicated times post-administration, *Plasmodium* nuclei were stained with Hoechst 33342 before proceeding to microscopic observation. The negative control was a blood sample taken just before polymer administration. DIC: differential interference contrast. Scale bar: 10 μm.

possibility is suggested by previous preliminary data obtained with curcumin loaded in liposomes formed by the anionic copolymer Eudragit® S100 and the water-soluble dextrin Nutriose® FM06 (Eudragit-nutriosomes). When Eudragit-nutriosomes containing <4% curcumin were orally administered to *P. yoelii yoelii*-infected mice at a dose of 75 mg curcumin kg^{-1} day^{-1}, mice survival was increased from 6 to 11 days relative to free drug [13]. Future research should explore the counterintuitive possibility that reducing curcumin load might increase the antimalarial efficacy of orally administered PBMA-MESBMA.

4. Conclusion

The membranes of *Plasmodium*-infected red blood cells are relatively complex due to numerous parasite proteins that are exported to them and little research has been done regarding how this modification of its plasma membrane affects the permeability of the erythrocyte to nanoparticles. The results presented here suggest that a zwitterionic character might impart polymeric nanocarriers the capacity for trespassing pRBC membranes. The zwitterionic polymer PBMA-MESBMA in particular targets and enters pRBCs in vivo following oral administration to malaria-infected mice. One mg of this polymer can incorporate and solubilize up to 0.3 mg of the lipophilic compound curcumin, a property that could be applied to improve the plasma concentration of other antimalarial drugs with low aqueous solubility. PBMA-MESBMA-based nanoparticles could be developed into a molecular shuttle capable of quickly rising pRBC-targeting hydrophobic antimalarial drug amounts in plasma following oral administration.

Supplementary data to this article can be found online at https://doi.

org/10.1016/j.jconrel.2021.01.028.

Funding

This research was funded by the *Ministerio de Ciencia, Innovación y Universidades*, Spain; grant number RTI2018–094579-B-I00 (which included FEDER funds), by the *Secretaria d'Universitats i Recerca* of the *Departament d'Empresa i Coneixement* of the *Generalitat de Catalunya*, and by the European Social Fund (2019 FI_B2 00165).

Declaration of Competing Interest

None.

Acknowledgments

ISGlobal and IBEC are members of the CERCA Programme, *Generalitat de Catalunya*. We acknowledge support from the Spanish Ministry of Science, Innovation and Universities through the *"Centro de Excelencia Severo Ochoa 2019-2023"* Program (CEX2018–000806-S). This research is part of ISGlobal's Program on the Molecular Mechanisms of Malaria which is partially supported by the *Fundación Ramón Areces*.

References

[1] P. Urbán, J.J. Valle-Delgado, E. Moles, J. Marques, C. Díez, X. Fernàndez-Busquets, Nanotools for the delivery of antimicrobial peptides, Curr. Drug Targets 13 (2012) 1158–1172.
[2] P. Urbán, X. Fernàndez-Busquets, Nanomedicine against malaria, Curr. Med. Chem. 21 (2014) 605–629.
[3] N. Kuntworbe, N. Martini, J. Shaw, R. Al-Kassas, Malaria intervention policies and pharmaceutical nanotechnology as a potential tool for malaria management, Drug Dev. Res. 73 (2012) 167–184.
[4] E. Moles, S. Galiano, A. Gomes, M. Quiliano, C. Teixeira, I. Aldana, P. Gomes, X. Fernàndez-Busquets, ImmunoPEGliposomes for the targeted delivery of novel lipophilic drugs to red blood cells in a falciparum malaria murine model, Biomaterials 145 (2017) 178–191.
[5] E. Moles, K. Moll, J.H. Ch'ng, P. Parini, M. Wahlgren, X. Fernàndez-Busquets, Development of drug-loaded immunoliposomes for the selective targeting and elimination of rosetting *Plasmodium falciparum*-infected red blood cells, J. Control. Release 241 (2016) 57–67.
[6] P. Urbán, J. Estelrich, A. Adeva, A. Cortés, X. Fernàndez-Busquets, Study of the efficacy of antimalarial drugs delivered inside targeted immunoliposomal nanovectors, Nanoscale Res. Lett. 6 (2011) 620.
[7] P. Urbán, J. Estelrich, A. Cortés, X. Fernàndez-Busquets, A nanovector with complete discrimination for targeted delivery to *Plasmodium falciparum*-infected versus non-infected red blood cells *in vitro*, J. Control. Release 151 (2011) 202–211.
[8] J. Marques, E. Vilanova, P.A.S. Mourão, X. Fernàndez-Busquets, Marine organism sulfated polysaccharides exhibiting significant antimalarial activity and inhibition of red blood cell invasion by *Plasmodium*, Sci. Rep. 6 (2016) 24368.
[9] J. Marques, J.J. Valle-Delgado, P. Urbán, E. Baró, R. Prohens, A. Mayor, P. Cisteró, M. Delves, R.E. Sinden, C. Grandfils, J.L. de Paz, J.A. García-Salcedo, X. Fernàndez-Busquets, Adaptation of targeted nanocarriers to changing requirements in antimalarial drug delivery, Nanomedicine: NBM 13 (2017) 515–525.
[10] J. Marques, E. Moles, P. Urbán, R. Prohens, M.A. Busquets, C. Sevrin, C. Grandfils, X. Fernàndez-Busquets, Application of heparin as a dual agent with antimalarial and liposome targeting activities toward *Plasmodium*-infected red blood cells, Nanomedicine: NBM 10 (2014) 1719–1728.
[11] E. Martí Coma-Cros, A. Biosca, J. Marques, L. Carol, P. Urbán, D. Berenguer, M. C. Riera, M. Delves, R.E. Sinden, J.J. Valle-Delgado, L. Spanos, I. Siden-Kiamos, P. Pérez, K. Paaijmans, M. Rottmann, A. Manfredi, P. Ferruti, E. Ranucci, X. Fernàndez-Busquets, Polyamidoamine nanoparticles for the oral administration of antimalarial drugs, Pharmaceutics 10 (2018) 225.
[12] P. Urbán, J.J. Valle-Delgado, N. Mauro, J. Marques, A. Manfredi, M. Rottmann, E. Ranucci, P. Ferruti, X. Fernàndez-Busquets, Use of poly(amidoamine) drug conjugates for the delivery of antimalarials to *Plasmodium*, J. Control. Release 177 (2014) 84–95.
[13] E. Martí Coma-Cros, A. Biosca, E. Lantero, M.L. Manca, C. Caddeo, L. Gutiérrez, M. Ramírez, L.N. Borgheti-Cardoso, M. Manconi, X. Fernàndez-Busquets, Antimalarial activity of orally administered curcumin incorporated in Eudragit®-containing liposomes, Int. J. Mol. Sci. 19 (2018) 1361.
[14] D. Campoccia, L. Montanaro, C.R. Arciola, A review of the biomaterials technologies for infection-resistant surfaces, Biomaterials 34 (2013) 8533–8554.
[15] B.D. Ratner, S.J. Bryant, Biomaterials: where we have been and where we are going, Annu. Rev. Biomed. Eng. 6 (2004) 41–75.
[16] M. Lundqvist, J. Stigler, T. Cedervall, T. Berggård, M.B. Flanagan, I. Lynch, G. Elia, K. Dawson, The evolution of the protein corona around nanoparticles: a test study, ACS Nano 5 (2011) 7503–7509.
[17] D. Walczyk, F.B. Bombelli, M.P. Monopoli, I. Lynch, K.A. Dawson, What the cell "sees" in bionanoscience, J. Am. Chem. Soc. 132 (2010) 5761–5768.
[18] Y.Y. Wang, S.K. Lai, J.S. Suk, A. Pace, R. Cone, J. Hanes, Addressing the PEG mucoadhesivity paradox to engineer nanoparticles that "slip" through the human mucus barrier, Angew. Chem. Int. Ed. Engl. 47 (2008) 9726–9729.
[19] S.K. Lai, D.E. O'Hanlon, S. Harrold, S.T. Man, Y.Y. Wang, R. Cone, J. Hanes, Rapid transport of large polymeric nanoparticles in fresh undiluted human mucus, Proc. Natl. Acad. Sci. U. S. A. 104 (2007) 1482–1487.
[20] R.A. Cone, Barrier properties of mucus, Adv. Drug Deliv. Rev. 61 (2009) 75–85.
[21] A.A. Date, J. Hanes, L.M. Ensign, Nanoparticles for oral delivery: design, evaluation and state-of-the-art, J. Control. Release 240 (2016) 504–526.
[22] E. Blanco, H. Shen, M. Ferrari, Principles of nanoparticle design for overcoming biological barriers to drug delivery, Nat. Biotechnol. 33 (2015) 941–951.
[23] K. Knop, R. Hoogenboom, D. Fischer, U.S. Schubert, Poly(ethylene glycol) in drug delivery: pros and cons as well as potential alternatives, Angew. Chem. Int. Ed. Engl. 49 (2010) 6288–6308.
[24] S. Guo, L. Huang, Nanoparticles escaping RES and endosome: challenges for siRNA delivery for cancer therapy, J. Nanomater. 2011 (2011) 742895.
[25] A. Hamilton, L. Biganzoli, R. Coleman, L. Mauriac, P. Hennebert, A. Awada, M. Nooij, L. Beex, M. Piccart, I. Van Hoorebeeck, P. Bruning, D. de Valeriola, EORTC 10968: a phase I clinical and pharmacokinetic study of polyethylene glycol liposomal doxorubicin (Caelyx®, Doxil®) at a 6-week interval in patients with metastatic breast cancer, Ann. Oncol. 13 (2002) 910–918.
[26] J.M. Harris, R.B. Chess, Effect of pegylation on pharmaceuticals, Nat. Rev. Drug Discov. 2 (2003) 214–221.
[27] M.C. Parrott, J.M. DeSimone, Drug delivery: relieving PEGylation, Nat. Chem. 4 (2011) 13–14.
[28] A. Herrmann, L. Pratsch, K. Arnold, G. Lassmann, Effect of poly(ethylene glycol) on the polarity of aqueous solutions and on the structure of vesicle membranes, Biochim. Biophys. Acta Biomembr. 733 (1983) 87–94.
[29] O. Tirosh, Y. Barenholz, J. Katzhendler, A. Priev, Hydration of polyethylene glycol-grafted liposomes, Biophys. J. 74 (1998) 1371–1379.
[30] F.K. Bedu-Addo, L. Huang, Interaction of PEG-phospholipid conjugates with phospholipid: implications in liposomal drug delivery, Adv. Drug Deliv. Rev. 16 (1995) 235–247.
[31] P. Zhang, F. Sun, S. Liu, S. Jiang, Anti-PEG antibodies in the clinic: current issues and beyond PEGylation, J. Control. Release 244 (Pt B) (2016) 184–193.
[32] F.M. Veronese, Peptide and protein PEGylation: a review of problems and solutions, Biomaterials 22 (2001) 405–417.
[33] L. Zhang, Z. Cao, T. Bai, L. Carr, J.R. Ella-Menye, C. Irvin, B.D. Ratner, S. Jiang, Zwitterionic hydrogels implanted in mice resist the foreign-body reaction, Nat. Biotechnol. 31 (2013) 553–556.
[34] J.T. Huckaby, S.K. Lai, PEGylation for enhancing nanoparticle diffusion in mucus, Adv. Drug Deliv. Rev. 124 (2018) 125–139.
[35] L. Zheng, H.S. Sundaram, Z. Wei, C. Li, Z. Yuan, Applications of zwitterionic polymers, React. Funct. Polym. 118 (2017) 51–61.
[36] J. Wu, W. Lin, Z. Wang, S. Chen, Y. Chang, Investigation of the hydration of nonfouling material poly(sulfobetaine methacrylate) by low-field nuclear magnetic resonance, Langmuir 28 (2012) 7436–7441.
[37] J. Wu, S. Chen, Investigation of the hydration of nonfouling material poly(ethylene glycol) by low-field nuclear magnetic resonance, Langmuir 28 (2012) 2137–2144.
[38] S. Chen, L. Li, C. Zhao, J. Zheng, Surface hydration: principles and applications toward low-fouling/nonfouling biomaterials, Polymer 51 (2010) 5283–5293.
[39] S. Jiang, Z. Cao, Ultralow-fouling, functionalizable, and hydrolyzable zwitterionic materials and their derivatives for biological applications, Adv. Mater. 22 (2010) 920–932.
[40] J.B. Schlenoff, Zwitteration: coating surfaces with zwitterionic functionality to reduce nonspecific adsorption, Langmuir 30 (2014) 9625–9636.
[41] A. Laschewsky, Structures and synthesis of zwitterionic polymers, Polymers 6 (2014) 1544–1601.
[42] S. Liu, S. Jiang, Zwitterionic polymer-protein conjugates reduce polymer-specific antibody response, Nano Today 11 (2016) 285–291.
[43] B. Li, Z. Yuan, H.C. Hung, J. Ma, P. Jain, C. Tsao, J. Xie, P. Zhang, X. Lin, K. Wu, S. Jiang, Revealing the immunogenic risk of polymers, Angew. Chem. Int. Ed. Engl. 57 (2018) 13873–13876.
[44] B. Li, J. Xie, Z. Yuan, P. Jain, X. Lin, K. Wu, S. Jiang, Mitigation of inflammatory immune responses with hydrophilic nanoparticles, Angew. Chem. Int. Ed. Engl. 57 (2018) 4527–4531.
[45] S.S. Olmsted, J.L. Padgett, A.I. Yudin, K.J. Whaley, T.R. Moench, R.A. Cone, Diffusion of macromolecules and virus-like particles in human cervical mucus, Biophys. J. 81 (2001) 1930–1937.
[46] W.M. Saltzman, M.L. Radomsky, K.J. Whaley, R.A. Cone, Antibody diffusion in human cervical mucus, Biophys. J. 66 (1994) 508–515.
[47] W. Shan, X. Zhu, W. Tao, Y. Cui, M. Liu, L. Wu, L. Li, Y. Zheng, Y. Huang, Enhanced oral delivery of protein drugs using zwitterion-functionalized nanoparticles to overcome both the diffusion and absorption barriers, ACS Appl. Mater. Interfaces 8 (2016) 25444–25453.
[48] P. Anand, A.B. Kunnumakkara, R.A. Newman, B.B. Aggarwal, Bioavailability of curcumin: problems and promises, Mol. Pharm. 4 (2007) 807–818.
[49] R.A. Sharma, W.P. Steward, A.J. Gescher, Pharmacokinetics and pharmacodynamics of curcumin, in: B.B. Aggarwal, Y.J. Surh, S. Shishodia (Eds.), The Molecular Targets and Therapeutic Uses of Curcumin in Health and Disease, Springer US, Boston, MA, 2007, pp. 453–470.

[50] A. Shehzad, S. Khan, O. Shehzad, Y.S. Lee, Curcumin therapeutic promises and bioavailability in colorectal cancer, Drugs Today (Barc) 46 (2010) 523–532.
[51] K. Jain, S. Sood, K. Gowthamarajan, Modulation of cerebral malaria by curcumin as an adjunctive therapy, Braz. J. Infect. Dis. 17 (2013) 579–591.
[52] P.N. Mimche, D. Taramelli, L. Vivas, The plant-based immunomodulator curcumin as a potential candidate for the development of an adjunctive therapy for cerebral malaria, Malar. J. 10 (2011) S10.
[53] D.N. Nandakumar, V.A. Nagaraj, P.G. Vathsala, P. Rangarajan, G. Padmanaban, Curcumin-artemisinin combination therapy for malaria, Antimicrob. Agents Chemother. 50 (2006) 1859–1860.
[54] R.C. Reddy, P.G. Vatsala, V.G. Keshamouni, G. Padmanaban, P.N. Rangarajan, Curcumin for malaria therapy, Biochem. Biophys. Res. Commun. 326 (2005) 472–474.
[55] S.L. Cranmer, C. Magowan, J. Liang, R.L. Coppel, B.M. Cooke, An alternative to serum for cultivation of *Plasmodium falciparum in vitro*, Trans. R. Soc. Trop. Med. Hyg. 91 (1997) 363–365.
[56] C. Lambros, J.P. Vanderberg, Synchronization of *Plasmodium falciparum* erythrocytic stages in culture, J. Parasitol. 65 (1979) 418–420.
[57] D.A. Fidock, P.J. Rosenthal, S.L. Croft, R. Brun, S. Nwaka, Antimalarial drug discovery: efficacy models for compound screening, Nat. Rev. Drug Discov. 3 (2004) 509–520.
[58] W. Lin, Z. Wang, S. Chen, Zwitterionic polymers for targeted drug delivery, in: Y. Shen (Ed.), Functional Polymers for Nanomedicine, The Royal Society of Chemistry, 2013, pp. 227–244.
[59] A.B. Lowe, C.L. McCormick, Synthesis and solution properties of zwitterionic polymers, Chem. Rev. 102 (2002) 4177–4190.
[60] V. Hildebrand, A. Laschewsky, M. Päch, P. Müller-Buschbaum, C.M. Papadakis, Effect of the zwitterion structure on the thermo-responsive behaviour of poly (sulfobetaine methacrylates), Polym. Chem. 8 (2017) 310–322.
[61] A.B. Lowe, C.L. McCormick, Stimuli responsive water-soluble and amphiphilic (co) polymers, in: C.L. McCormick (Ed.), Stimuli-Responsive Water Soluble and Amphiphilic Polymers, American Chemical Society, Washington, DC, 2000, pp. 1–13.
[62] A.B. Lowe, M. Vamvakaki, M.A. Wassall, L. Wong, N.C. Billingham, S.P. Armes, A. W. Lloyd, Well-defined sulfobetaine-based statistical copolymers as potential antibioadherent coatings, J. Biomed. Mater. Res. 52 (2000) 88–94.
[63] World Health Organization. *Guidelines for the Treatment of Malaria*, 3rd edition. http://apps.who.int/iris/bitstream/10665/162441/1/9789241549127_eng.pdf. 2015. Geneva, Switzerland, World Health Organization.
[64] M.A. Travassos, M.K. Laufer, Resistance to antimalarial drugs: molecular, pharmacological and clinical considerations, Pediatr. Res. 65 (2009) 64R–70R.
[65] L. Cui, S. Mharakurwa, D. Ndiaye, P.K. Rathod, P.J. Rosenthal, Antimalarial drug resistance: literature review and activities and findings of the ICEMR network, Am. J. Trop. Med. Hyg. 93 (2015) 57–68.
[66] M. Delves, D. Plouffe, C. Scheurer, S. Meister, S. Wittlin, E. Winzeler, R.E. Sinden, D. Leroy, The activities of current antimalarial drugs on the life cycle stages of *Plasmodium*: a comparative study with human and rodent parasites, PLoS Med. 9 (2012), e1001169.
[67] M.J. Boyle, J.S. Richards, P.R. Gilson, W. Chai, J.G. Beeson, Interactions with heparin-like molecules during erythrocyte invasion by *Plasmodium falciparum* merozoites, Blood 115 (2010) 4559–4568.
[68] J.J. Valle-Delgado, P. Urbán, X. Fernàndez-Busquets, Demonstration of specific binding of heparin to *Plasmodium falciparum*-infected vs non-infected red blood cells by single-molecule force spectroscopy, Nanoscale 5 (2013) 3673–3680.
[69] J. Movellan, P. Urbán, E. Moles, J.M. de la Fuente, T. Sierra, J.L. Serrano, X. Fernàndez-Busquets, Amphiphilic dendritic derivatives as nanocarriers for the targeted delivery of antimalarial drugs, Biomaterials 35 (2014) 7940–7950.
[70] E. Moles, P. Urbán, M.B. Jiménez-Díaz, S. Viera-Morilla, I. Angulo-Barturen, M. A. Busquets, X. Fernàndez-Busquets, Immunoliposome-mediated drug delivery to *Plasmodium*-infected and non-infected red blood cells as a dual therapeutic/prophylactic antimalarial strategy, J. Control. Release 210 (2015) 217–229.